Available online at www.sciencedirect.com
ScienceDirect
Inorganica Chimica Acta 361 (2008) 2195–2202
Inorganica Chimica Acta
www.elsevier.com/locate/ica

Synthesis, characterization and ethylene polymerization activity of titanium aminopyridinato complexes

Markku Talja [a,*], Tommi Luhtanen [b], Mika Polamo [a], Martti Klinga [a], Tapani A. Pakkanen [b], Markku Leskelä [a]

[a] Department of Chemistry, Laboratory of Inorganic Chemistry, University of Helsinki, P.O. Box 55, Helsinki, FIN-00014, Finland
[b] Department of Chemistry, University of Joensuu, P.O. Box 111, 80101 Joensuu, Finland

Received 29 March 2007; received in revised form 14 November 2007; accepted 20 November 2007
Available online 18 April 2008

Abstract

Three titanium complexes derived from 2-(2,6-difluoroanilino)pyridine and 2-(2-chloroanilino)pyridine were synthesized and characterized by X-ray diffraction or spectroscopic methods. All titanium complexes have been used to catalyze the polymerization of ethylene in the presence of MAO as cocatalyst. The mono(2,6-difluorophenylaminopyridinato) titanium catalyst was found to be more active in ethylene polymerization than the bis(2,6-difluorophenylaminopyridinato) and bis(2-chlorophenylaminopyridinato) titanium catalysts. *ortho*-Halogens disturbed the β-elimination transition state of ethylene polymerization and formed higher molar mass polyethylene than their unhalogenated congener. Due to fluxionality, the bis(2-chlorophenylaminopyridinato) titanium catalyst formed broader molar mass distribution than the bis(2,6-difluorophenylaminopyridinato) titanium catalysts.

Keywords: Crystal structure; Titanium; Aminopyridine; Amidopyridine; Aminopyridinato; Polyethylene

1. Introduction

In recent years, an increasing number of aminopyridine metal complexes have been studied due to the established catalytical polymerization activity of this class of compounds and novel structural features presented by the metal complexes of such ligands [1,2]. Moreover, the ligating properties of nitrogen containing amidinates and aminopyridines and their metal complexes have been extensively studied [3–10]. The present study is a continuation of our work on the coordination chemistry of aminopyridine derivatives [9]. This work has been extended to the hitherto uninvestigated 2-(2,6-difluoroanilino)pyridine and 2-(2-chloroanilino)pyridine complexes of titanium because we hypothesized previously that more unstable complexes should also be more active in ethylene polymerization. Halogen substituents at *ortho*/*para* position of the phenyl group of the phenylaminopyridine should affect the titanium center through mesomeric effect (Fig. 1). Field effect, i.e. the interaction of the *ortho*-fluorine or -chlorine with titanium may involve a C–X···Ti bonding and compete with pyridine coordination and hence affect ethylene polymerization (Fig. 2) [11,12].

In this work, we compare the catalytic activity of complexes with *ortho*-fluorides or -chlorides in the phenyl group of the aminopyridinato titanium complex. By comparing the structures of halogenated phenylaminopyridinato titanium complexes and their unsubstituted phenylaminopyridinato titanium complexes in ethylene polymerization it should be possible to differentiate the mesomeric or field effect on the catalyst because usually electron donating ligands produce a longer molar mass than electron withdrawing ligands (Figs. 1 and 2). The possibility that the *ortho*-halogen interacts electronically with a β-H on a growing polymer chain leading to enhanced molar masses will be considered [13]. We will also study by molecular modeling calculations how the stabilities of the different

* Corresponding author. Tel.: +358 9 191 50223; fax: +358 9 191 50198.
E-mail address: markku.talja@helsinki.fi (M. Talja).

0020-1693/$ - see front matter © 2007 Elsevier B.V. All rights reserved.
doi:10.1016/j.ica.2007.11.028

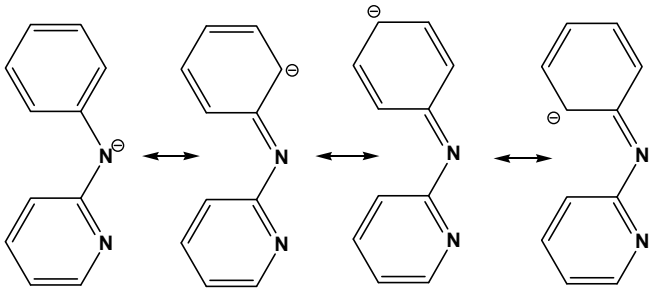

Fig. 1. Resonance structures of the phenyl group of the phenylamidopyridine.

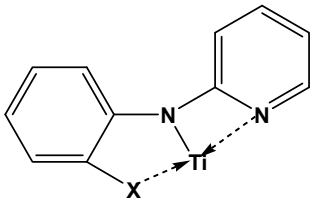

Fig. 2. The plausible C–X···Ti interaction competes with internal pyridine coordination.

configurations of the complexes and catalysts correlate with ethylene polymerization activities.

2. Experimental

All the complexation reactions were done under argon using standard Schlenk techniques. Solvents were dried and distilled before use. NMR spectra were recorded at 200 MHz on a Varian Gemini 200 spectrometer; $CDCl_3$ as solvent, TMS as an internal standard. IR spectra were obtained on a Perkin–Elmer 1000 spectrophotometer.

All complexes were analyzed with TGA/SDTA at normal pressure in nitrogen atmosphere.

Mass spectra were recorded with a JEOL JMS-SX102 operating in the electron impact mode (70 eV).

IR spectra in a range 4000–400 cm^{-1} were measured from KBr tablets and in a range 710–30 cm^{-1} from Nujol mull on polystyrene film. The KBr was dried in an oven before use. The KBr tablets were prepared in a glove box under argon. The proligands, 2-(2-chlorophenylamino)pyridine and 2-(2,6-difluorophenylamino)pyridine, were performed as described in the literature [15,16].

2.1. Synthesis

General procedure for preparing bis(amidopyridinato) titanium complexes. Aminopyridine ligand was let to react with NaH (excess) in dry Et_2O (40 ml) at room temperature until no gas was evolved. The yellow ether solution of sodium amidopyridine was filtrated through glass filter and added drop wise to the orange toluene solution of $TiCl_4$ (5 mmol in 40 ml) and stirred 1 h at room temperature. The reaction mixture was filtrated through Kieselguhr and the solvent volume was reduced under vacuum to approximately 30 ml. The dark red crystals suitable for X-ray measurements were obtained overnight.

2.1.1. Data of $C_{22}H_{14}Cl_2F_4N_4Ti$ (*1*)

Yield g, 89%. ^1H NMR ($CDCl_3$, 200 MHz): 7.89 (d, 2H, H_6), 7.49 (ddd, 2H, H_4), 7.18–6.89 (m, 6H), 6.60 (ddd, 2H, H_5), 6.15 (d, 2H, H_3).

^{13}C NMR: 165.69 (C_2), 156.06 (d) ($C_{9/13}$), 141.97 (C_6), 141.88 (C_4), 128.59 (d) (C_8), 126.39 (t) (C_8), 114.84 (C_5), 111.87 (d) ($C_{10/12}$), 105.17 (C_3).

EI mass spectrum: m/z (relative intensity) 529 (M^+, 17), 410 (26), 281 (40), 206 (95), 186 (100).

IR (KBr): $v = 1648$(m), 1597(s), 1495(s), 1473(s), 1458(s), 1445(s), 1209(m), 1004(s), 652(w), 280(m) cm^{-1}.

Anal. Calc. for $C_{22}H_{14}Cl_2F_4N_4Ti$: C, 49.94; H, 2.67; N, 10.59. Found: C, 49.41; H, 2.87; N, 10.13%.

2.1.2. Data of $C_{22}H_{14}Cl_6F_4N_4Ti_2$ (*2*)

Yield g, 96%. ^1H NMR ($CDCl_3$, 200 MHz): 7.98 (d, 2H, H_6), 7.57 (ddd, 2H, H_4), 7.27–7.00 (m, 6H), 6.68 (ddd, 2H, H_5), 6.18 (d, 2H, H_3).

^{13}C NMR: 165.51 (C_2), 151.98(d) ($C_{9/13}$), 142.17 (C_6), 140.41 (C_4), 128.17(d) (C_8), 124.73(t), 117.27 (C_5), 111.76 (d) ($C_{10/12}$), 103.46 (C_3).

EI mass spectrum: m/z (relative intensity) 648 (6), 528 (4), 358 (13), 323 (5), 270 (28), 235 (13), 206 (96), 186 (100).

IR (KBr): $v = 1645$(s), 1616(s), 1597(s), 1472(s), 1384(m), 1171(m), 1007(s), 785(s), 760(s), 654(w), 284(m), 279(m), 273(m) cm^{-1}.

Anal. Calc. for $C_{22}H_{14}Cl_6F_4N_4Ti$: C, 36.76; H, 1.96; N, 7.79. Found: C, 35.99; H, 2.33; N, 6.97%.

2.1.3. Data of $C_{22}H_{16}Cl_4N_4Ti$ (*3*)

Yield g, 87%. ^1H NMR ($CDCl_3$, 200 MHz): 7.99 (dt, 1H, H_6), 7.50 (ddd, 1H, H_4), 7.34–7.03 (m, 4H), 6.68 (1H, ddd, H_5), 6.03 (dt, 1H, H_3).

^{13}C NMR ($CDCl_3$) δ: 165.54 (C_2), 145.67 (C_6), 142.13 (C_4), 141.85 (C_8), 129.83 (C_{10}), 127.68 (C_{12}), 127.54 (C_9), 127.33 (C_{11}), 127.00 (C_{13}), 114.86 (C_5), 105.64 (C_3).

Anal. Calc. for $C_{22}H_{16}Cl_4N_4Ti$: C, 50.20; H, 3.10; N, 10.60. Found: C, 49.90; H, 3.55; N, 10.15%.

EI mass spectrum: m/z (relative intensity) 526 (M^+, 6), 491 (4), 232 (12), 204 (21), 169 (100).

IR (KBr): $v = 1647$(m), 1595(s), 1472(s), 1457(s), 1444(s), 1213(m), 757(s), 658(w), 280(w) cm^{-1}.

2.2. Structure determination and refinement

Structures were solved with the SHELXTL 5.1 program package using direct methods that showed the positions of the non-hydrogen atoms. Further refinement with full-matrix least squares on F^2 was carried out with SHELXL 97 using all collected reflections. Non-hydrogen atoms were refined anisotropically. Hydrogen atoms were introduced into calculated positions.

2.3. Theoretical calculations

Geometry optimizations were performed at the HF/3-21G* level, which has been shown to provide reliable structures for group 4 transition-metal complexes, especially for titanium-based complexes. Based on our earlier studies, neither increasing the size of the basis set nor inclusion of electron correlation at the MP2 level has a significant influence on the geometries, but would certainly increase calculation times. Single-point MP2 calculations were performed to confirm the relative stability order of the conformations of the studied titanium complexes. At the single-point calculations, basis set 6-31G* for C, H, and N and equal-level generated basis set for Ti were used. The stability orders, produced by both methods, are generally in good agreement with each other. The geometry minima were confirmed by frequency calculations. All calculations were carried out by the GAUSSIAN 03 program package [14].

2.4. Polymerization experiments

See reference [9].

3. Results

Pro-ligands were synthesized using 2-chloropyridine and hydrogen chloride of 2-monochloroaniline or 2,6-difluoroaniline [15,16]. The bis(2,6-difluorophenylaminopyridinato) and bis(2-chlorophenylaminopyridinato) titanium complexes were synthesized by using the same procedure as for bis(phenylaminopyridinato) titanium complex [17]. The ligand precursor, 2-arylaminopyridine, was treated with 1 equiv. of sodium hydride in Et_2O. The deprotonated ligand in Et_2O was added into the toluene solution of $TiCl_4$. An immediate color change from yellow and orange to purple indicated a rapid reaction. After the filtration of the reaction mixture, complex **1** was obtained with a good yield as a dark purple solid material (Fig. 3). Complex **3** was synthesized in a similar manner. This reaction was selective and the ligand to metal ratio can be controlled easily. Complex **2** was synthesized as described earlier for $\{Ti[PhNpy]Cl_3\}_2$ [9].

3.1. IR-spectra

When aminopyridinato ligand is involved in metal bonding, some changes appear in IR-spectrum and these changes are expected in the IR spectra of complexes **1**– **3**. A comparison between the spectra of the free ligand with those of its chelates reveals that considerable changes in frequencies have occurred due to chelation. The general features of the IR spectra of complexes **1**–**3** are similar in nature. When pyridine ring nitrogen involves in complex formation, certain ring modes increase in value because of the coupling with the $Ti–N_{py}$ bond vibrations and alterations of the ring force field. In the solid state the peak at 1652 cm^{-1} of complex **1**, $(2,6\text{-}F_2Ap)_2TiCl_2$, indicates the chelation due to the coordination of pyridine to titanium because this absorption is assigned to the C=N stretching mode shifting the stretching to a higher frequency. The IR spectra of complex **1**–**3** do not show the characteristic ν(N–H) band which was observed in the free ligand lending further support to the suggestion that the ligand is coordinated to titanium. In the plane deformation of NH at 1524 cm^{-1} has also disappeared.

Furthermore, the IR spectrum of complex **1** in KBr showed three very strong bands at 1597, 1472, and 1004 cm^{-1}. The first two are assigned to C–N stretchings and the last one indicated the C–F vibration, respectively. Also, three strong bands at 1496, 1458, and 1444 are all attributed to pyridine coordinated to the titanium. The retention of vibration of fluoro substituents at 1004 cm^{-1} indicates that there is no interaction between titanium and fluorine in complex **1**. The titanium–nitrogen vibrations of complex **1** can be seen at 708 and 652 cm^{-1}. The metal chloride vibrations can be seen in the far IR region at 280 cm^{-1} indicating *cis*-configuration of the chlorides.

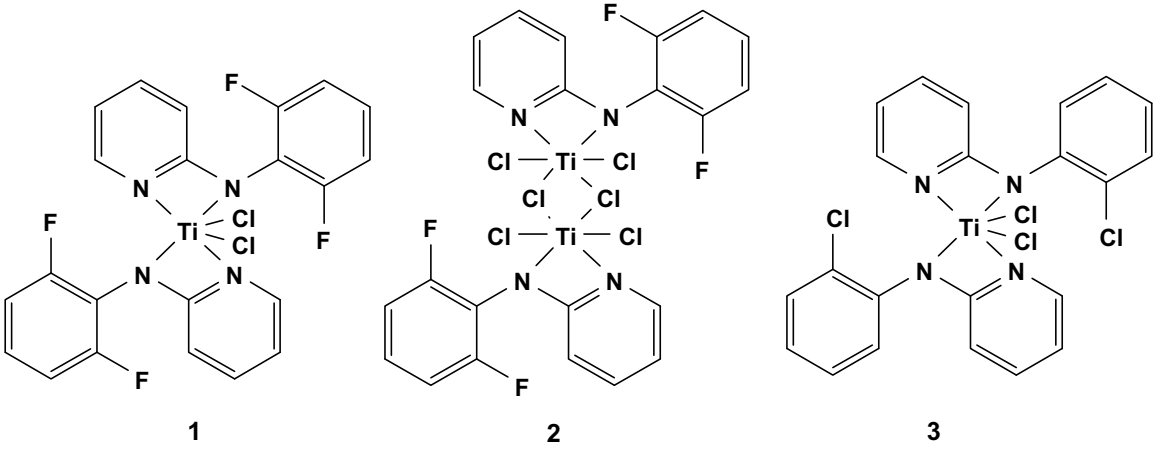

Fig. 3. Structures of titanium aminopyridinato precatalysts **1**–**3**.

Complex **2**, $[(2,6\text{-}F_2Ap)TiCl_3]_2$, has similar absorptions to those of complex **1**. They can be distinguished from complex **1** by the peaks at 716 and 700 cm^{-1}, which are assigned to titanium–nitrogen vibrations. Also, titanium–chloride vibrations are indicative because complex **2** has three peaks around 280 cm^{-1} but there is only one peak for complex **1**.

Complex **3**, $(2\text{-}ClAp)_2TiCl_2$, showed indicative peaks at 1647, 1457, and 1444 cm^{-1} due to pyridine coordination to titanium as complex **1**. Also, C–N stretching at 1595 and 1472 cm^{-1} are comparable to complex **1**. The absorptions around 700 and at 280 cm^{-1} are the same within resolution than for complex **1**, the former implying Ti–N vibrations and the latter *cis*-dichloro configuration of the octahedral titanium complex.

3.2. Mass spectra

The mass spectrum of complex **1** has molecular ion at *m*/*z* 529 corresponding to monomeric complex $(2,6\text{-}F_2Ap)_2TiCl_2$. Two different fragmentation routes can be seen in the spectrum, the loss of chlorine atom (*m*/*z* 493) and the loss of $TiCl_2$ (*m*/*z* 410) neutral fragment. However, the loss of two chlorine atoms cannot be seen.

In the mass spectrum of complex **2**, the highest mass peak (*m*/*z* 718) cannot be seen but the loss of Cl_2 can be seen at *m*/*z* 648. Although the peak at *m*/*z* 358 points to the monomeric $(2,6\text{-}F_2Ap)TiCl_3$ complex the peaks at *m*/*z* 648 and *m*/*z* 528 ($(2,6\text{-}F_2Ap)TiCl_3$–$TiCl_4$) indicates the dimeric complex as in the case of $[ApTiCl_3]_2$ [9].

The molecular ion peak of complex **3** was observed at *m*/*z* 526 in its mass spectrum confirming its formula weight and monomeric nature. The fragmentation pattern of the complex showed a fragment at *m*/*z* 206 due to the 2-ClAp-ligand. Also, fragments were shown at *m*/*z* 321 and 491, which were assigned to the loss of 2-chloroanilinopyridine ligand and chloride, respectively. Clearly, the complex **3** has two fragmentation routes as with the complex **1**.

3.3. NMR-spectra

The ^1H NMR spectrum of complex **1** comprises two spin systems, a four-proton for the pyridine group and a three-proton system for the 2, 6-difluoroaniline residue. All the signals are in the unsaturated region indicating solvent free complexes. Complex **1** shows six magnetically and chemically different protons indicating time-averaged molecular C_2-symmetry. The doublet of α-proton to $N_{pyridine}$ can be seen at 7.89 ppm in the ^1H NMR spectrum which is shielded from that of free ligand (8.19 ppm) and correspondingly in the ^{13}C NMR spectrum C_2 is deshielded by 5 ppm indicating coordination of titanium to amidopyrine moiety at 165.7 ppm. This shielding effect is typical of aminopyridinato coordinated to early transition metals. In principle, the binding mode can be purely amido metal bond (Fig. 4A) or a delocalized resonance hybrid (D) based on resonance structures (B or C). Comparing with other known aminopyridinato works, the NMR data indicates structure B in solution.

Complex **2** has almost identical ^1H NMR spectrum to complex **1**. The shielding effect of complex **2** is not so pronounced than in complex **1**. The highest signal of assigned proton H_6 can be seen at 7.98 ppm in complex **2**. In the ^{13}C NMR spectrum, the C_2 shows the signal at 165.5 ppm.

Complex **3** comprises two spin systems, a four-proton for the pyridine residue and a four-proton system for the 2-chloroaniline residue. The highest signal in the ^1H NMR spectrum, the doublet of H_6 can be seen at 7.99 ppm and in the ^{13}C NMR spectrum the chemical shift of C_2 at 165.5 ppm.

3.4. Crystal structure

The solid state structure of complex **1** consists of a titanium atom surrounded by two aminopyridinato ligands and two chlorine atoms (Fig. 5). Complex **1** has C_2 symmetry bisecting the Cl1–Ti–Cl2 angle. The titanium center has distorted octahedral geometry. Four nitrogen atoms and two chloride atoms define the coordination sphere of titanium. The main reason for the distorted octahedral geometry in complex **1** is the two substantially narrow four-membered chelate rings, N1–Ti–N7 and N14–Ti–N20 are 63.26(8)° and 63.39(8)°, respectively (Table 1). The Cl1–Ti–Cl2 angle is 100.54(3)°, which is wider than that in Ap_2TiCl_2 (97.03(5)°) [9]. The Ti–N_{py}, Ti–N_{amide}, and Ti–Cl bond distances of complex **1** are similar to those in known aminopyridinato titanium complexes (Table 1).

Complex **1** differs from the unsubstituted parent compound, bis(phenylaminopyridinato) titanium complex [9], by different configurations in that complex **1** has pyridine rings close to each other and fluorosubstituted phenyl rings are situated as far away as possible. Complex **1** is *Δ-cis,-trans,cis* and the unsubstituted phenylaminopyridinato is *Δ*/*Λ-cis,cis,cis* when CIP (Cahn–Ingold–Prelog) priority is $N_{py} > N_{amide} > Cl$ [6]. The configuration of complex **1** can be explained by the fact that electronegative fluoro sub-

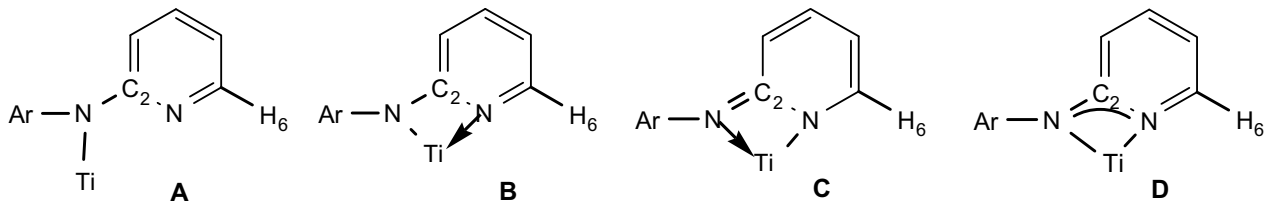

Fig. 4. Binding modes of titaniumaminopyridinato complex.

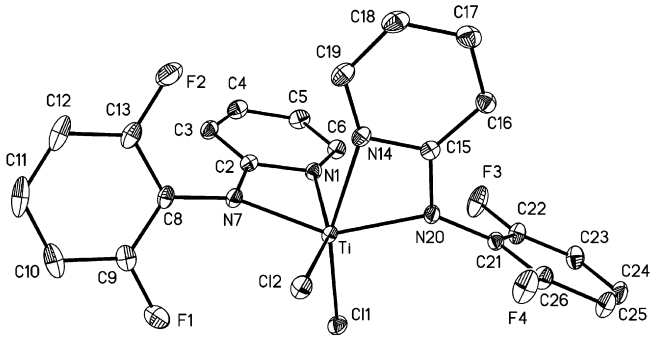

Fig. 5. Crystal structure of complex **1**. Hydrogen atoms are omitted for clarity. The thermal ellipsoids correspond to 30% probability.

Table 1
Selected bond lengths (Å) and angles (°) for complex **1**

Ti1–N1	2.174(2)	N1–Ti1–N20	94.00(8)
Ti1–N7	2.029(2)	N7–Ti1–Cl1	106.17(7)
Ti1–N14	2.192(2)	N7–Ti1–Cl2	92.81(6)
T1–N20	2.029(2)	N7–Ti1–N14	91.09(8)
Ti1–Cl1	2.2679(8)	N7–Ti1–N20	148.09(9)
Ti1–Cl2	2.2838(8)	N14–Ti1–Cl1	159.21(6)
		N14–Ti1–Cl2	89.87(6)
N1–Ti1–Cl1	92.42(6)	N14–Ti1–N20	63.39(8)
N1–Ti1–Cl2	155.33(6)	N20–Ti1–Cl1	96.32(6)
N1–Ti1–N7	63.26(8)	N20–Ti1–Cl2	105.21(6)
N1–Ti1–N14	83.97(8)	Cl1–Ti1–Cl2	100.54(3)

stituents are oriented in a way that they are as far apart from each other as possible and that amido nitrogens form the shortest bonds to the titanium. Also, C13–C8–N7–C2 torsion angle is 62.2° (corresponding angle in the free ligand at solid state = 121.8°) indicating that the resonance structure shown in Fig. 1 is not valid because no shortening of N_{amide}–C_{aryl}-bond can be seen. Electronic factors, including the *trans*-influence and π-donor properties of the ligands, are likely to influence the structures of the complexes **1** and **2**. According to configuration analysis of $(bidentate)_2MX_2$ complexes by Kepert [18], *cis*-X structures are preferred and this is the case for complex **1** but not for the parent phenylaminopyridinato complex [9].

3.5. Thermogravimetry

The thermal stabilities of the titanium aminopyridinato complexes were studied because they are 16 electron complexes and they should show some sort of instability during the heating. The thermal behavior of four aminopyridinato complexes Ap_2TiCl_2 (**4**), $(2,6\text{-}F_2Ap)_2TiCl_2$ (**1**), $(2\text{-}ClAp)_2TiCl_2$ (**3**) and $(2,6\text{-}F_2Ap)TiCl_3$ (**2**) was followed by TGA in nitrogen atmosphere (Fig. 6). All complexes seem to evaporate since the amount of decomposition residue is only 5% in case of $(2,6\text{-}F_2Ap)_2TiCl_2$ (**1**), $(2,6\text{-}F_2Ap)TiCl_3$ (**2**) and Ap_2TiCl_2 (**4**) and 15% in case of $(2\text{-}ClAp)_2TiCl_2$ (**3**). As usual, the mono(aminopyridinato) titanium complex showed higher volatility than the bis(aminopyridinato) titanium complexes. In case of $(2\text{-}ClAp)_2TiCl_2$ the

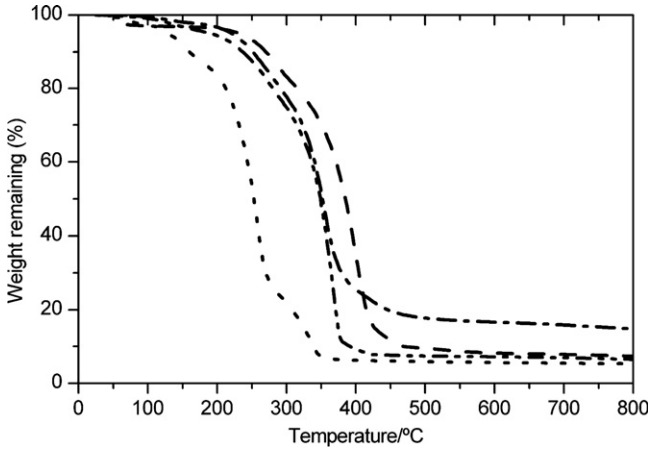

Fig. 6. Thermogravimetric curves for $(2\text{-}ClAp)_2TiCl_2$ (———), Ap_2TiCl_2 (——), $(2,6\text{-}F_2Ap)_2TiCl_2$ (—·-·—), $(2,6\text{-}F_2Ap)TiCl_3$ (---).

higher amount of residue indicates that it also decomposes. It is difficult to say what the decomposition mechanism is since the weight of the residue corresponds to titanium oxide. Because the heating is carried out in nitrogen the residue cannot be pure oxide but most obviously carbon or nitrogen containing material. This indicates that the Ap ligand is strongly bonded to the titanium center and reveals that the Ap_2Ti unit is very stable. In view of these observations, we assumed that d^0 Ap_2TiR^+ species should be reasonably stable and should coordinate ethylene *cis* to the Ti–R bond because the *cis*-X structures are usually the most stable ones [2,19,20].

On the basis of X-ray, IR, NMR, MS, and TG measurements the compounds **1** and **3** form monomeric *cis*-dichloro octahedral complexes. For complex **2**, a dimeric structure with symmetric chloro bridges is proposed. These data are related to that previously described aminopyridinato complexes [21–23].

3.6. Modeling

The stability of $TiMe^+$ complexes was modeled and compared with the cationic form of $TiCl_4$ to find correlation between complex structure and polymerization behavior. Table 2 shows the relative energies of the

Table 2
The relative stability energies E_{Rel} of the dichloro complexes $E_{rel}(Cl_2)$ and their cationic forms $E_{Rel}(TiMe^+)$ including different isomer structures

Complex	E_{Rel} (Cl_2)	E_{Rel} ($TiMe^+$)	Relative stability of cationic form (kJ/mol)
$(2,6\text{-}F_2Ap)_2TiCl_2$*cis,cis,cis* (**1**)	0.0	0.0	−402
$(2,6\text{-}F_2Ap)_2TiCl_2$*cis,trans,cis* (**1**)	−19.2	16.5	−367
$(2,6\text{-}F_2Ap)TiCl_3$ (**2**)			−312
$(2\text{-}ClAp)_2TiCl_2$*cis,cis,cis* (**3**)	0.0	0.0	−360
$(2\text{-}ClAp)_2TiCl_2$*cis,trans,cis* (**3**)	8.1	−11.1	−380
Ap_2TiCl_2*cis,cis,cis* (**4**)	0.0	0.0	−345
Ap_2TiCl_2*cis,trans,cis* (**4**)	7.3	−1.7	−354
$TiCl_4$			0

configurations of the dichloride (Cl_2) and cationic forms ($TiMe^+$). In the case of complex **1** and **3**, the *cis*,*cis*,*cis* configurations are favorable in dichloro forms. Complex **2** favors the *cis*,*trans*,*cis* configuration in dichloro form. The cationic forms behaved on the contrary *i.e.* complexes **1** and **3** prefers *cis*,*trans*,*cis* configurations and complex **2** favors the *cis*,*cis*,*cis* configuration. A similar kind of situation has been obtained for bis(salicylamidinato) titanium dichloro system [24]. This kind of behavior might explain why the activities are only moderate because the cationic form adopts the less active configuration. Moreover, the stability of cationic forms should affect the activity of the catalyst and the molar mass distribution of the produced polymer.

The last column of Table 2 shows the relative stability of cationic forms compared with $TiCl_4$. The activity order according to the calculations is $TiCl_4 > (2,6\text{-}F_2Ap)TiCl_3$ (**2**) > Ap_2TiCl_2 (**4**) > $(2\text{-}ClAp)_2TiCl_2$ (**3**) > $(2,6\text{-}F_2Ap)_2TiCl_2$ (**1**) which differs from the measured activities only in order of the last two complexes (*vide infra*). It seems that the smaller the relative value, the more active is the catalyst. The activity versus the relative stability of the cationic form correlates positively. This indicates that the more stable the cationic form, the less active it is in polymerization. The correlation has to be regarded qualitative, since the stabilities are on a relative scale, and other factors influence the catalytic activity of the complex.

3.7. Polymerization results

The polymerization activities of the catalyst precursors **1**–**3** were studied in the ethylene polymerization. Cationic catalysts were generated by the reaction of the corresponding complexes with methylaluminoxane (MAO). As summarized in Table 3, the ethylene polymerization activity order is **2** > **4** > **1** > **3**. Thus, for the aminopyridinato titanium complexes, the electron withdrawing groups do not have a beneficial effect on activity. With halogen substituted bis(aminopyridinato) titanium complexes **1** and **3**, the molar masses increased in comparison with the unhalogenated congener (**4**, Run 9). Interestingly, complex **1** has molar mass, molar mass distribution and crystallinity twice than that with complex **2** (Runs 1 and 3). The *ortho*-chloride or -fluoride at phenylaminopyridinato titanium catalyst decreases the rate of polymerization and opposes β-hydride elimination resulting in longer polymer chains. Steric bulk increases the termination barrier and increases the molar mass of the polymer but the steric factors also decrease the activity of the catalysts. In case of aminopyridinato catalysts fluoro or chloro substituents provide no living polymerization character as seen in bis(phenoxy-imine) catalysts [13]. Considering that the molar mass is determined by the relative rates of chain propagation and chain termination the fluoride substituted phenylaminopyridinato catalysts **1** exhibits higher chain propagation rates than **4** unlike in the case of pyridyldiamine catalysts [11]. *ortho*-Chloro substituent in $(2\text{-}ClAp)_2TiCl_2$ (**3**) lead to the several active species resulting in the wide molar mass distribution (Run 8). In the further examination, the most active titanium catalyst, $2,6\text{-}F_2ApTiCl_3$ (**2**), behaved according to the expectations when the temperature and pressure were changed (Runs 2–6) but Run 7 had surprisingly high molar mass.

4. Discussion

Steric factors have a dramatic effect on the decrease in the activity of aminopyridinato catalysts. The addition of the first aminopyridine ligand decreases the activity to the one tenth compared with the activity of $TiCl_4$/MAO (Runs 3 and 10). The addition of the second aminopyridine ligand does not affect the decrease in the activity as significantly (Runs 1, 8 and 9). The activity decreased in order $TiCl_4 > (2,6\text{-}F_2Ap)TiCl_3 > Ap_2TiCl_2 > (2,6\text{-}F_2Ap)_2\ TiCl_2 > (2\text{-}ClAp)_2TiCl_2$ due to stericity.

Electronic factors from molecular modeling results indicates that the low activities of bis(aminopyridinato) titanium catalysts compared with mono(aminopyridinato) titanium catalyst were attributed to more stable cationic species. If the cation is too stable, ethylene coordination

Table 3
Results of ethylene polymerizations promoted by complexes **1**–**4** and $TiCl_4$ with MAO[a]

Run	Cat.[a]	T_p (°C)	P_p (bar C_2H_4)	Activity (kg PE mol^{-1} Ti^{-1} h^{-1})	M_w (g mol^{-1})	M_w/M_n	T_m[b] (°C)	X_c%[c]
1	$(2,6\text{-}F_2Ap)_2TiCl_2$ (**1**)	60	5	67	604000	4.5	136.7	57
2	$(2,6\text{-}F_2Ap)TiCl_3$ (**2**)	60	3	61	351000	2.1	132.9	5
3	$(2,6\text{-}F_2Ap)TiCl_3$ (**2**)	60	5	133	309000	2.7	134.5	29
4	$(2,6\text{-}F_2Ap)TiCl_3$ (**2**)	60	7	338	541000	2.2	133.0	32
5	$(2,6\text{-}F_2Ap)TiCl_3$ (**2**)	80	6	448	465000	2.7	134.6	65
6	$(2,6\text{-}F_2Ap)TiCl_3$ (**2**)	80	7	552	367000	6.3	135.6	55
7	$(2,6\text{-}F_2Ap)TiCl_3$ (**2**)	80	8	640	1392000	6.9	133.2	26
8	$(2\text{-}ClAp)_2TiCl_2$ (**3**)	60	5	56	344000	12.4	135.9	41
9	Ap_2TiCl_2[d] (**4**)	60	5	95	239000	2.4	133.4	56
10	$TiCl_4$[d]	60	5	1112	15000	8.6	127.4	57

[a] Polymerization conditions: [Al]:[Ti] = 3000:1; n_{cat} = 10 μmol; t_p = 1 h.
[b] Melting point determined by DSC. These values have been obtained from remelted samples at a heating rate of 10 °C/min.
[c] X_c (%): Crystallinity = $100(\Delta H_m/\Delta H_m^*)$; $\Delta H_m^* = 290$ J/g.
[d] Values differ from previous work because of remeasured sample [9].

into the ion-pair will not be favorable and the concentration of ethylene complex remains low. The more electron deficient metal complex usually indicates the less active catalyst leading to a strong electronic interaction between the ethylene and metal center and hence the higher insertion activation barrier. Mono(aminopyridinato) titanium complexes possess a more electrophilic and sterically open nature compared with bis(aminopyridinato) titanium complexes but mono(aminopyridinato) titanium catalysts display higher ethylene polymerization activities than bis(aminopyridinato) titanium catalysts. The activity behavior of $ApTiCl_3$ and Ap_2TiCl_2 in the polymerization of the ethylene was reported earlier [9].

It is generally agreed that the substituent which donates electrons to the metal center leads to increase in the length of the polymer chain [25]. The use of the electron donor ligands should give a longer polymer chain than electron acceptor ligands. The difluoroaniline is clearly an electron acceptor, that is, it should reduce the chain propagation. According to the polymerization results, the (2,6-F_2Ap)$TiCl_2$ catalyst doubles the growth of the polymer chain length compared with its non substituted congener (Runs 1 and 9). Furthermore, one 2,6-F_2Ap ligand raises the molar mass 29%, whereas two 2,6-F_2Ap ligands raise the molar mass 150% with respect to the molar mass of Ap_2TiCl_2/MAO (Runs 3 and 9). According to this logic, the titanium metal centre must get electron density from somewhere and it would be the most natural to suppose that the fluoride substituents interact with the metal centre through space. Another possibility is that the transition state usually has some resemblance to a hydride-bis(olefin) complex, *i.e.* there is direct interaction between titanium and the hydrogen being transferred. If the transition state of β-hydrogen interaction is disturbed and hence decreased, the higher molar mass could be expected. The fluorine atom in monoaminopyridinato (2,6-F_2Ap)$TiCl_3$/MAO-catalyst probably has not so many interaction possibilities with the titanium core or the β-hydrogen of the growing polymer chain than bis(aminopyridinato) (2,6-F_2Ap)$_2TiCl_2$/MAO catalysts.

Aminopyridinato is not a rigid system because the pyridine–titanium bond is able to open and the rotation of the ligand can take place around the amido-titanium bond. Rotation around the pyridine–amidonitrogen bond and the phenyl–amidonitrogen bond can also exist. The chlorine substituent of the aryl part slows down the rotation of the amidopyridinato ligand and that is why several active centres are found in the catalysis.

5. Conclusion

The titanium aminopyridinato complexes can be prepared in a controlled manner. The aminopyridinato chelate ring clearly confers stability to the complex as it was formed in a good yield when aminopyridine was added into $TiCl_4$ solution of toluene. The X-ray structure of bis(difluorophenylaminopyridinato) titanium precatalyst shows no interaction between the titanium center and the nearest fluorine atom in the solid state. We suggest that in solution fluoro and chloro substituents in aminopyridinato catalysts do not have pronounced electron withdrawing effect through bonds but the interaction between titanium and chloro/fluoro-substituents, *i.e.* Ti···XAr, reduces the electropositivity of the titanium center or disturbs the β-elimination transition state of ethylene polymerization.

Pyridine-alkoxides have fluxional behavior in solution and it is expected that also bis(aminopyridinates) undergo a structural change when they are activated with MAO [26–28]. This structural perturbation most probably stabilizes and reduces the activity of the catalyst. Thinking about the future work, steric crowding near the active centre restricts the polymerization process. If stericity can be moved farther from the active metal centre, in other words if the phenyl substituent is changed to benzyl substituent, the activity should also increase.

6. Supplementary material

CCDC 639707 contains the supplementary crystallographic data for this paper. These data can be obtained free of charge from The Cambridge Crystallographic Data Centre via www.ccdc.cam.ac.uk/data_request/cif.

Acknowledgements

This work was supported by the Finnish National Technology Agency (TEKES) and Borealis Polymers Oy.

References

[1] R. Kempe, Eur. J. Inorg. Chem. (2003) 791.
[2] R. Kempe, Angew. Chem., Int. Ed. 39 (2000) 468.
[3] E.J. Crust, I.J. Munslow, C. Morton, P. Scott, Dalton Trans. (2004) 2257.
[4] C. Morton, P. O'Shaughnessy, P. Scott, Chem. Commun. (2000) 2099.
[5] C. Jones, P.C. Junk, S.G. Leary, N.A. Smithies, Inorg. Chem. Commun. 6 (2003) 1126.
[6] E.J. Crust, A.J. Clarke, R.J. Deeth, C. Morton, P. Scott, Dalton Trans. (2004) 4050.
[7] N.M. Scott, T. Schareina, Oleg Tok, R. Kempe, Eur. J. Inorg. Chem. (2004) 3297.
[8] A. Noor, W. Kretschmer, R. Kempe, Eur. J. Inorg. Chem. (2006) 2683.
[9] M. Talja, M. Klinga, M. Polamo, E. Aitola, M. Leskelä, Inorg. Chim. Acta 358 (2005) 1061.
[10] M. Talja, M. Polamo, Polyhedron 25 (2006) 3039.
[11] R.R. Schrock, J. Adamchuck, K. Ruhland, L.P.H. Lopez, Organometallics 22 (2003) 5079.
[12] N. Adams, H.R. Bigmore, T.L. Blundell, C.L. Boyd, S.R. Dubberley, A.J. Sealey, A.R. Cowley, M.E.G. Skinner, P. Mountford, Inorg. Chem. 44 (2005) 2882.
[13] M. Mitani, J. Mohri, Y. Yoshida, J. Saito, S. Ishii, K. Tsuru, S. Matsui, R. Furuyama, T. Nakano, H. Tanaka, S. Kojoh, T. Matsugi, N. Kashiwa, T. Fujita, J. Am. Chem. Soc. 124 (2002) 3327.
[14] M.J. Frisch, G.W. Trucks, H.B. Schlegel, G.E. Scuseria, M.A. Robb, J.R. Cheeseman, J.A. Montgomery, T. Vreven Jr., K.N. Kudin, J.C. Burant, J.M. Milliam, S.S. Iyengar, J. Tomasi, V. Barone, B. Mennucci, M. Cossi, G. Scalmani, N. Rega, G.A. Petersson, H.

Nakatsuji, M. Hada, M. Ehara, K. Toyota, R. Fukuda, J. Hasegawa, M. Ishida, T. Nakajima, Y. Honda, O. Kitao, H. Nakai, M. Klene, X. Li, J.E. Knox, H.P. Hratchian, J.B. Cross, C. Adamo, J. Jaramillo, R. Gomperts, R.E. Stratmann, O. Yazyev, A.J. Austin, R. Cammi, C. Pomelli, J.W. Ochterski, P.Y. Ayala, K. Morokuma, G.A. Voth, P. Salvador, J.J. Dannenberg, V.G. Zakrzewski, S. Dapprich, A.D. Daniels, M.C. Strain, O. Farkas, D.K. Malick, A.D. Rabuck, K. Raghavachari, J.B. Foresman, J.V. Ortiz, Q. Cui, A.G. Baboul, S. Clifford, J. Cioslowski, B.B. Stefanov, G. Liu, A. Liashenko, P. Piskorz, I. Komaromi, R.L. Martin, D.J. Fox, T. Keith, M.A. Al-Laham, C.Y. Peng, A. Nanayakkara, M. Challacombe, P.M.W. Gill, B. Johnson, W. Chen, M.W. Wong, C. Gonzalez, J.A. Pople, Gaussian, Inc., Pittsburgh, PA, 2003.

[15] M. Talja, M. Polamo, Z. Kristallogr. NCS 220 (2005) 39.

[16] M. Polamo, M. Talja, Z. Kristallogr. NCS 219 (2004) 317.

[17] M. Talja, M. Klinga, M. Polamo, E. Aitola, M. Leskelä, Inorg. Chim. Acta 358 (2005) 1061.

[18] D.L. Kepert, in: S.L. Lippard (Ed.), Progress in Inorganic Chemistry, vol. 23, Wiley, New York, 1977, p. 1.

[19] C. Boisson, J.C. Berthet, M. Ephritikhine, M. Lance, M. Nierlich, J. Organomet. Chem. 531 (1997) 115.

[20] L. Scoles, R. Minhas, R. Duchateau, J. Jubb, S. Gambarotta, Organometallics 13 (1994) 4978.

[21] I. Westmoreland, I.J. Munslow, P. O'Shaughnessy, P. Scott, Organometallics 22 (2003) 2972.

[22] C. Jones, P.C. Junk, S.G. Leary, N.A. Smithies, Inorg. Chem. Commun. 6 (2003) 1126.

[23] H. Fuhrmann, S. Brenner, P. Arndt, R. Kempe, Inorg. Chem. 35 (1996) 6742.

[24] A. Pärssinen, T. Luhtanen, M. Klinga, T. Pakkanen, M. Leskelä, T. Repo, Eur. J. Inorg. Chem. (2005) 2100.

[25] I.-K. Lee, W.J. Gauthier, J.M. Ball, B. Iyenger, S. Collins, Organometallics 11 (1992) 2115.

[26] X. Bei, D.C. Swenson, R.F. Jordan, Organometallics 16 (1997) 3282.

[27] T. Tsukahara, D.C. Swenson, R.F. Jordan, Organometallics 16 (1997) 3303.

[28] I. Kim, Y. Nishihara, R.F. Jordan, R.D. Rogers, A.L. Rheingold, G.P.A. Yap, Organometallics 16 (1997) 3314.